Available online at www.sciencedirect.com

ScienceDirect

Ceramics International 41 (2015) S234–S239

CERAMICS INTERNATIONAL

www.elsevier.com/locate/ceramint

Comparative study of Mn^{3+} and Mn^{2+} doping effects on structure and electrical properties of $BiFeO_3$ thin films

Yinjuan Ren, Xiaohong Zhu*, Jiliang Zhu, Jianguo Zhu, Dingquan Xiao

Department of Materials Science, Sichuan University, Chengdu 610065, China

Received 26 October 2014; accepted 4 March 2015
Available online 2 April 2015

Abstract

$BiFeO_3$ (BFO) thin films doped differently with 5 mol% Mn^{3+} and 5 mol% Mn^{2+} were prepared on (111)Pt/Ti/SiO_2/Si substrates by a sol–gel method with rapid thermal annealing. Systematic analyses about the two different doping effects and their underlying mechanisms were performed. Pure and doped BFO films were well crystallized in perovskite structure, whilst doping of Mn^{3+} and Mn^{2+} resulted in slight distortion in the lattice structure. After doping, smaller grain size, diminished structural defects and denser microstructure were confirmed. Both Mn^{3+} and Mn^{2+} dopants could reduce the concentration of oxygen vacancies in BFO films, whereas Mn^{3+}doping exhibited better ability. As a result, the Mn^{3+} doped film showed the highest dielectric permittivity among those three samples, $\varepsilon_r = 105$ at 100 kHz; meanwhile, the Mn^{3+} doped film showed a superior $2P_r$ value of 79.5 μC/cm^2, compared to 63.2 μC/cm^2 for the Mn^{2+} doped film and unachievable intrinsic ferroelectric polarizations in the undoped BFO film because of high leakage contribution. The leakage current density in medium/high electric field region was dramatically decreased by Mn doping, accompanied with a change of conduction mechanism from the space charge limited conduction to the Schottky mechanism.

Keywords: C. Ferroelectric properties; Multivalent Mn dopant; $BiFeO_3$; Thin films

1. Introduction

As a typical single phase multiferroic material, $BiFeO_3$ (BFO) with its characteristics of large remanent polarization of $P_r \sim 100$ μC/cm^2 [1,2] and coexistence of ferroelectric and antiferromagnetic orderings at room temperature possesses the promising potential application in nonvolatile ferroelectric random access memory, transducer and spintronics [3–5]. In the past few years, both experimental and theoretical methods have been used to deeply study the structure, electrical and magnetic properties of BFO to push its practical use [1,6–8]. Unfortunately, the high leakage current mainly hinders the various applications [8,9]. It is widely accepted that oxygen vacancies caused by the redox coupling of Fe ions and the volatilization of Bi^{3+} primarily result in high leakage current, thus seriously deteriorating the ferroelectric properties of BFO films [10]. In order to decrease the leakage current and improve its electrical behavior, site engineering has been proposed and studied. Elements like Sm, Gd, Tb, Nd were introduced into A-site [11–13], and Mn, Co, Sc, Cr were used to replace B-site [14–16]. Among those ion substitutions, the film with Mn substitution exhibits a significantly reduced leakage current and an improved breakdown voltage, so that well-saturated ferroelectric hysteresis loops can be detected.

It is known that the element of manganese has several different valence states. Iron ions also reveal 2+ and 3+ in BFO films, and their respective percentages are associated with the level of oxygen vacancy amount, which finally affects the electrical properties of BFO films. Thus the effects of differently valenced Mn ion substitution on the valence states of Fe ions in BFO films will be very interesting, which may stimulate the variation of ferroelectric properties of BFO films. In the present work, Mn^{3+} and Mn^{2+} were separately introduced into the B-site of BFO films via a simple sol–gel spin-coating method. Their influences on crystallization, morphology and electrical

---

*Corresponding author. Tel.: +86 28 85412415; fax: +86 28 85416050.
E-mail addresses: xhzhu@scu.edu.cn, xhzhu2006@gmail.com (X. Zhu).

http://dx.doi.org/10.1016/j.ceramint.2015.03.269
0272-8842/

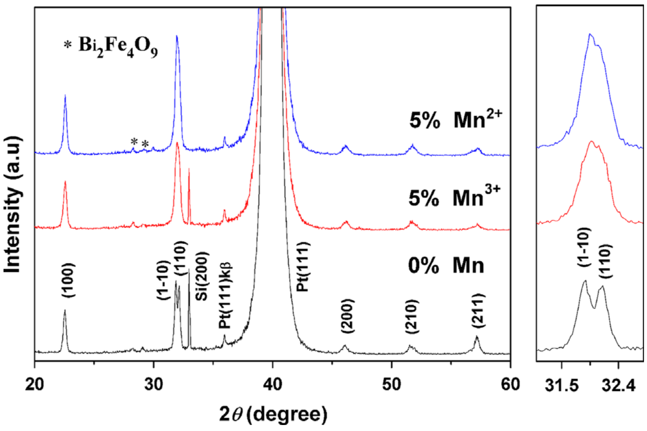

Fig. 1. XRD patterns of $BiFe_{0.95}M_{0.05}O_3$ ($M=Mn^{3+}$ and Mn^{2+}) and pure $BiFeO_3$ thin films deposited on (111)Pt/Ti/SiO_2/Si substrates. The right panel shows the magnified patterns in the vicinity of $2\theta=32°$.

properties have been comparatively investigated and analyzed. Meanwhile, the probable operating mechanisms on charge defects have been proposed to further understand the influences of different valences Mn substitution.

2. Experimental

$BiFe_{0.95}M_{0.05}O_3$ ($M=Mn^{3+}$ and Mn^{2+}) thin films were synthesized on (111)Pt/Ti/SiO_2/Si substrates via a simple sol–gel method with rapid thermal annealing. For Mn^{3+}, Mn^{2+} doped and pure $BiFeO_3$ thin films, except for different dopants, all the experimental parameters were the same. Firstly, as starting materials, bismuth nitrate [$Bi(NO_3)_3 \cdot 5H_2O$] and iron nitrate [$Fe(NO_3)_3 \cdot 9H_2O$] were dissolved in the mixed solution of prevailing 2-methoxyethanol and a small amount of acetic acid by magnetic stirring. The stirring time for early stage is 1 h to make bismuth nitrate and iron nitrate to thoroughly dissolve, and then a certain amount of manganese acetates [$C_6H_9MnO_6 \cdot 2H_2O$] and [$C_4H_6MnO_4 \cdot 4H_2O$] were separately added to the two solutions. After all the three solutions have been stirred for another 11 h, we finally obtained the stoichiometric solutions of 5 mol% Mn^{3+}, 5 mol% Mn^{2+} doped and pure $BiFeO_3$ thin films. Considering the volatilization of Bi during an annealing process, Bi $(NO_3)_3 \cdot 5H_2O$ was weighed with 5 mol% excess, so the mole ratio of bismuth nitrate and iron nitrate was 1.05:1. All the solutions were prepared in an ambient atmosphere at room temperature.

The following deposition processes were performed in a clean room. To begin with, the three as-prepared fresh sols were spin-coated on the cleaned substrates via a rotation rate of 3000 rpm for 20 s. Then, in order to remove volatile materials, the wet films were put on the hot plates of 80 °C for 5 min and subsequently 180 °C for 5 min. After that, the three films were annealed through a rapid thermal process. At this stage, the films were annealed at 715 °C for 90 s with a heating rate of 5 °C/s in air. What is more, every layer was annealed after spin coating and the thickness of single layer was approximately 50 nm. For the purpose of electrical performance characterization, top electrodes of 0.00071 cm^2 were sputtered on the surfaces of films through a shadow mask designed by us. Finally, the deposited top electrodes were annealed at 300 °C for 10 min to make the electrodes and films get full contact.

X-ray diffraction (XRD, DX-2700, Dandong, China), operating at 40 kV, 30 mA with Cu Kα radiation, was utilized to characterize the crystalline phase of those three films. In order to analyze the microstructure of films, surface and cross section morphologies were detected by a field-emission scanning electron microscope (FESEM, JSM-7500F, JEOL, Japan). Besides, X-ray photoelectron spectroscopy (XPS, AXIS UItra DLD, KRATOS, Britain) was used to investigate the compositions of thin films and the combination states of Fe 2p and Mn 2p electrons, where the spectrum of Fe was fitted to calculate the quantity ratio of Fe^{2+} and Fe^{3+}. As for electrical properties studies, the dielectric constant (ε_r) and loss tangent (tan δ) of films were identified by an HP 4294A impedance analyzer. The ferroelectric polarization versus electric field (P–E) hysteresis loop and leakage current density were measured using a Radiant ferroelectric test system. All the measurement processes above were carried out at room temperature.

3. Results and discussion

The XRD patterns of $BiFe_{0.95}M_{0.05}O_3$ and $BiFeO_3$ thin films scanned (2θ value) from 20° to 60° are shown in Fig. 1. As marked by "*" in Fig. 1, a slight $Bi_2Fe_4O_9$ impurity phase was detected for all the films annealed at 715 °C in air. We attribute that to a higher annealing temperature of 715 °C, as compared to 700 °C in our previous work [17], which formed single pure structure in $BiFeO_3$ thin films. Meanwhile, it confirms that the sintering temperature influences the formation of stoichiometric $BiFeO_3$ and other secondary phases associated with dynamics of $BiFeO_3$ phase formation. Nonetheless, because of the denser microstructure and superior electrical properties in the 715 °C annealed BFO film, 715 °C was further accepted to explore the effects of different valence states of Mn doping. All the prominent peaks in XRD plots match well with perovskite structure as $BiFeO_3$ with a degree of (110) preferred orientation. Even though no evident differences on lattice structure between Mn^{3+} and Mn^{2+} doped films were observed, Mn doping really induced a slight distortion in the lattice structure. In the magnified patterns shown on the right side of Fig. 1, in the vicinity of 32°, (110) and ($1\bar{1}0$) reflections were clearly separated for the undoped $BiFeO_3$ film, indicating the perovskite structure with rhombohedral symmetry. For the Mn-doped films, however, reflection peak ($1\bar{1}0$) weakened and overlapped with peak (110). It can be then inferred that by Mn doping, the distorted rhombohedral structure of parent BFO film was amended toward the orthorhombic or tetragonal structure [18].

In Fig. 2(a), the cross-sectional image of 5 mol% Mn^{3+}-doped film detected by FESEM verified the good contact between deposited film and bottom Pt electrode without apparent diffusion and clear segregation. Not only for the Mn^{3+}-doped film, but also for the Mn^{2+}-doped and pure BFO films, the thickness is homogeneous and identified to be approximately 300 nm. Fig. 2